Agricultural Water Management 243 (2021) 106459

Contents lists available at ScienceDirect

Agricultural Water Management

journal homepage: www.elsevier.com/locate/agwat

Thermal Crop Water Stress Index Base Line Temperatures for Sugarbeet in Arid Western U.S

B.A. King[a,*], D.D. Tarkalson[a], V. Sharma[b], D.L. Bjorneberg[a]

[a] USDA-ARS, Northwest Irrigation and Soil Research Laboratory, 3793 N 3600 E, Kimberly, ID, 83341-5076, USA
[b] Agricultural and Biological Engineering Department, University of Florida, P.O. Box 110570, Gainesville, 32606, FL, USA

ARTICLE INFO

Keywords:
sugarbeet
canopy temperature
irrigation scheduling
water stress

ABSTRACT

Sugarbeet is a deep-rooted crop in unrestricted soil profiles that can readily utilize stored soil water to reduce seasonal irrigation requirements. Soil water below 0.6 m is not commonly considered for irrigation scheduling due to the labor and expense of soil water monitoring at deeper depths and uncertainty in effective rooting depth and soil water holding capacity. Thermal-based crop water stress index (CWSI) irrigation scheduling for sugarbeet has the potential to overcome soil water monitoring limitations and facilitate utilization of stored soil water. In this study, canopy temperature of irrigated sugarbeet under full irrigation (FIT) and 25%FIT in 2014, 2015, 2017 and 2018 in southcentral Idaho and FIT and 60%FIT in 2018 in northwestern Wyoming USA was monitored from full cover through harvest along with meteorological conditions and soil water content. A neural network (NN) was used to predict well-watered canopy temperature based on 15-min average values for solar radiation, air temperature, relative humidity, and wind speed collected -1 to +2.5 hours of solar noon (13:00 – 16:00 MDT). A linear regression driven physical model for estimating the difference between a non-transpiring canopy and air temperature resulted in a value of 13.7 ˚C for the meteorological conditions of the study. A daily CWSI value calculated as the average 15-min CWSI calculated between 13:00 and 16:00 MDT was well correlated with irrigation amounts and timing. The daily CWSI value provided a more responsive indication of crop water stress than soil water monitoring in deficit irrigation treatments. The methodology used to calculate a daily CWSI could be used in irrigation scheduling to utilize soil water storage without knowledge of soil depth, crop rooting depth, or deep (> 0.6 m) soil water monitoring.

1. Introduction

With irrigated agriculture being the largest water consumer in the western U.S., increasing water resource use demands by non-agricultural users, and increasing variable regional and seasonal precipitation, it is vital that irrigated agriculture adopt new methods and management practices that increase water use efficiency while sustaining profitable farm enterprises. A key element of efficient irrigation management is optimum timing of irrigations or irrigation scheduling. Irrigation scheduling should be correlated with water use of the crop to minimize over-irrigation and unintended crop water stress. Conventional soil water balance-based scheduling relies on tracking estimated crop evapotranspiration (ET), maintaining a numerical soil water balance, and irrigating when available soil water is forecast to reach a predetermined lower limit based on known soil water holding capacity and crop effective root zone depth (Melvin and Yonts, 2009). Soil water content monitoring is necessary to periodically validate/adjust the numerical soil water balance to minimize errors. Irrigation scheduling can also be based on soil water monitoring alone and irrigating when a predetermined lower limit is approached (Vellidis et al., 2007).

Sugarbeet, a biennial crop for seed production and annual crop for sugar production, is known to have a deep root system resulting from its long vegetative growth (Dunham, 1993). The rooting depth of sugarbeet cited in the irrigation management literature ranges from 0.7 to 2.0 m (Withers and Vipond, 1980; James, 1988; Jensen et al., 1990; Dunham, 1993; Martin et al., 2007). Winter (1980) reported soil water extraction to permanent wilting point to a depth of 3 m across ten irrigation treatments. In the absence of soil depth limitations and depending on soil water holding capacity, sugarbeet can access a large soil water reservoir allowing the use of stored winter precipitation to reduce seasonal irrigation water use. The potential deep rooting characteristic

* Corresponding author.
E-mail addresses: brad.king@usda.gov (B.A. King), david.tarkalson@usda.gov (D.D. Tarkalson), vsharma1@ufl.edu (V. Sharma), dave.bjorneberg@usda.gov (D.L. Bjorneberg).

https://doi.org/10.1016/j.agwat.2020.106459
Received 11 September 2019; Received in revised form 4 August 2020; Accepted 17 August 2020
0378-3774/ Published by Elsevier B.V.

of sugarbeet limits the practicality of soil water measurement for irrigation scheduling in commercial sugarbeet production due to the time and/or equipment availability or costs. Limiting soil water monitoring to practical depths (< 0.6 m) precludes the exploitation of deeper soil water to reduce seasonal irrigation requirements, however, the potential impact on yield is unknown and needs to be evaluated.

Plant canopy temperature monitoring provides an attractive alternative to soil water-based irrigation scheduling. Water stress promotes stomatal closure, reducing transpirational cooling and increasing leaf temperature (Raschke, 1960; Tanner, 1963). Infrared radiometers have been used to measure plant canopy temperature under field conditions to estimate evapotranspiration and drought stress in many crops (Maes and Steppe, 2012). Canopy temperature measurement of fully sunlit leaves near solar noon for irrigation scheduling expressed as a simple empirical relationship called the crop water stress index (CWSI) was proposed by Idso et al. (1981) and Jackson et al. (1981). The CWSI is a linear index ranging from 0 when under identical climatic conditions measured canopy temperature (T_c) is equal to well-watered canopy temperature (T_{LL}) and 1 when T_c is equal to non-transpiring canopy temperature (T_{UL}). Temperatures T_{LL} and T_{UL} are lower and upper baselines used to normalize CWSI for the effects of atmospheric conditions (air temperature, relative humidity, solar radiation, wind speed, etc.) on transpiration and canopy temperature. Ideally, CWSI ranges from 0 to 1 where 0 represents a well-watered condition and 1 represents a non-transpiring, severely water-stressed condition. Practical application of CWSI based irrigation scheduling has been limited by the difficulty of estimating T_{LL} and T_{UL} (Maes and Steppe, 2012). Theoretical determination of crop specific constants for T_{LL} and T_{UL} relative to ambient air temperature has not been fruitful due to the poorly understood and complex influences of canopy architecture and environmental conditions on the soil–plant–air continuum (Idso et al., 1981; Jones, 1999; Jones, 2004; Payero and Irmak, 2006). In the original development and application of the CWSI, T_{LL} and T_{UL} were experimentally determined from the linear correlation between T_c-T_a and vapor pressure deficit (VPD) using measured T_c on well-watered experimental plots to account for major climatic effects confounding T_c measurements and hindering determination of water stress status (Idso, 1982). Use of well-watered control plots to determine T_{LL} and T_{UL} is not practical in commercial agriculture nor is it possible to maintain a crop canopy under non-transpiring conditions. Alternative methods of estimating T_{LL} and T_{UL} have been investigated including use of artificial wet and dry reference surfaces (Jones, 1999; Jones et al., 2002; Leinonen and Jones, 2004; Cohen et al., 2005; Alchanatis et al., 2010; O'Shaughnessy et al., 2011; Pou et al., 2014). The required maintenance of the artificial surfaces limits potential use for maintenance free automation in the commercial crop production environment.

Data-driven empirical methods to estimate T_{LL} and T_{UL} have been investigated in scientific studies. Payero and Irmak (2006) used multiple linear regression (MLR) with independent variables T_a, solar radiation (R_s), crop height, wind speed (WS), and VPD or relative humidity (RH) to estimate T_{LL} corn and soybean with correlation coefficients of 0.69–0.84 between the predicted and measured canopy temperature. Irmak et al. (2000) determined for water-stressed corn that T_{UL} was 4.6–5.1 °C above air temperature. In several subsequent studies with crops other than corn, a value of air temperature plus 5.0 °C has been used for T_{UL} (Cohen et al., 2005; Möller et al., 2007; Alchanatis et al., 2010). O'Shaughnessy et al. (2011) used maximum daily air temperature plus 5.0 °C for T_{UL} of soybean and cotton. King and Shellie (2016) also obtained good results in estimating T_{LL} using MLR for wine grapes. They used T_a + 15 °C for T_{UL} based on the cumulative distribution of measured T_c-T_a of deficit irrigated wine grapes. King and Shellie (2016) also evaluated the use of artificial neural network (NN) models for estimating T_{LL} of wine grape with better results than MLR. While data driven methods to estimate T_{LL} have been successful, reliable estimation of T_{UL} has been more problematic in part due to the difficulty in achieving and maintaining a non-transpiring canopy for temperature data collection. Jackson et al. (1981) proposed an energy balance-based relationship for T_{UL}-T_c of a non-transpiring canopy as:

$$T_{UL} - T_a = \frac{r_a R_n}{\rho C_p} \tag{1}$$

where r_a is the canopy aerodynamic resistance (s m^{-1}), ρ is the density of air (kg m^{-3}), c_p is the heat capacity of air (J kg^{-1} °C^{-1}), and R_n is net radiation (W m^{-2}). The values in Eqn. 1 can be readily measured with exception of r_a to estimate T_{UL}. Direct estimation of r_a requires periodic field measurement of crop height and estimation of additional aerodynamic parameters (Bockhold et al., 2011). Alternately, O'Toole and Real (1986) proposed a methodology for estimating average r_a by representing the canopy energy balance relationship of Jackson et al. (1981) as a linear regression equation of T_c-T_a and VPD. They proposed using average values for the remaining variables as a practical means for estimating the regression coefficients. The resulting relationship for average canopy aerodynamic resistance ($\bar{r}_{ap}$) was:

$$\bar{r}_{ap} = \frac{\bar{\rho} C_p a}{\bar{R}_n b\left(\bar{\Delta} + {}^{1}/_{b}\right)} \tag{2}$$

where $\bar{R}_n$ is average R_n, $\bar{\Delta}$ is average is the slope of the water saturation vapor pressure-air temperature relation, (Pa °C^{-1}), $\bar{\rho}$ is average ρ and a and b are the intercept and slope regression coefficients, respectively. Substituting $\bar{r}_{ap}$ for r_a and $\bar{R}_n$ for R_n with measured T_a in Eqn. 1 allows for estimating T_{UL}. This physical approach to estimating T_{UL} does not require additional crop physical measurements other than a data set of well-watered canopy temperature and common meteorological measurements. Han et al. (2018) used this approach of estimating T_{UL} to compute a CWSI adjusted soil water balance for water-stressed maize with good results.

The objective of this study was to use NN modeling and the data-driven approach of O'Toole and Real (1986) to estimate T_{LL} and T_{UL}, respectively, for irrigated sugarbeet in the arid western U.S. and investigate the performance of CWSI values calculated using these estimates.

2. Materials and methods

2.1. Experimental sites

Sugarbeet plots were grown at two experimental sites, the USDA-ARS Northwest Irrigation and Soils Research Laboratory (NWISRL) near Kimberly, Idaho in 2014, 2015, 2017, and 2018, and the University of Wyoming Powell Research and Extension Center (PREC) in Powell, Wyoming in 2018. The NWISRL climate is arid where the 20-yr (1997-2016) average annual precipitation and alfalfa-reference ET are approximately 253 and 1479 mm, respectively, requiring irrigation for economical agricultural crop production. The PREC climate is also arid where the 29-yr (1981-2017) average annual precipitation and alfalfa-reference ET is approximately 166 mm and 1498 mm, respectively. Long-term (1981-2017) seasonal (May to September) average precipitation and alfalfa-reference ET are 144 mm and 988 mm, respectively, requiring irrigation for economical agricultural crop production. The soil at NWISRL is a Portneuf silt loam (coarse-silty mixed mesic Durixerollic Calciorthid and is classified as very deep and well drained with weak silica cementation ranging from 30 to 45 cm deep that may restrict root growth (USDA, 1998). The soil at PREC is a Garland loam (Fine-loamy over sandy or sandy-skeletal, mixed, superactive, mesic Typic Haplargids). The soil profile consists of loam changing to extremely gravelly loamy sand below 0.8 m that hinders soil sampling and soil water monitoring with a restrictive layer beyond 2.0 m (USDA, 2019)

2.2. Experimental Design

The field studies at both sites used a randomized block design with four replications at NWSIRL and three replications at PREC. In 2014 at NWISRL, the field study utilized one plot of a randomized block nitrogen fertilizer rate trial where all plots were fully irrigated (FIT). The FIT represented the condition where the sugarbeet crop was irrigated two or three times a week with a cumulative depth equal to weekly cumulative estimated evapotranspiration (ET). In 2015 at NWISRL, the field study utilized two replicates of a tillage trial with four irrigation treatments. The four irrigation treatments were FIT, 75% FIT, 50% FIT, and 25% FIT. In 2017 and 2018 at NWISRL, the field studies consisted of four replicates of the four irrigation treatments used in 2016. In 2018 at PREC, the field study consisted of three replicates of three irrigation treatments. The irrigation treatments were FIT, 75% FIT and 60% FIT. Lateral move or solid set sprinkler irrigation was used at NWISRL and lateral move irrigation was used at PREC. Local conventional sugarbeet cultural practices including 0.56 m row spacing were used at both experimental sites. Pesticides, herbicides, insecticides, and fungicides were applied to all plots uniformly when required.

2.3. Irrigation Scheduling and Soil Water Measurement

2.3.1. NWISRL - Kimberly, ID

In each study year irrigation scheduling for the FIT was based on balancing estimated cumulative weekly crop ET with the weekly cumulative irrigation and precipitation. Estimated crop ET based on 1982 Kimberly-Penman alfalfa reference evapotranspiration model and daily crop coefficients (Wright, 1982) was obtained from an Agrimet (U.S Bureau of Reclamation, https://www.usbr.gov/pn/agrimet/) weather station located within 4.5 km from the study site. Irrigation was applied 1 to 3 times a week depending upon weekly ET rate, less frequent at the beginning and end of the growing season. In 2015, 2016 and 2017, soil water content was measured in 0.15 m depth increments from 0.15 to 2.25 m using neutron probe calibrated to the experimental site soil using the methods of Hignett and Evett (2002). Soil water content in the 0 to 0.15 m depth was also continuously monitored using time domain reflectometery (TDR) (TDR 100, Campbell Scientific Co., Logan, UT) with two probes in the crop row. Soil water content was monitored in two replicated blocks in 2015 and four replicated blocks in 2017 and 2018. Soil water content using neutron probe was measured periodically throughout the growing season to avoid water stress in the fully irrigated treatments by ensuring that available soil water content remained greater than 45% of total available moisture (Jensen et al., 1990). Estimated well-watered sugarbeet ET between emergence and harvest, cumulative irrigation between emergence and harvest applied to the FIT and 25% FIT treatments in each study year at NWISRL are given in Table 1. The 25%FIT received 36, 50 and 42% of estimated sugarbeet ET in in 2015, 2017, and 2018, respectively.

Table 1
Estimated well-watered sugarbeet evapotranspiration (ET_c) between emergence and harvest, cumulative irrigation plus precipitation applied to the fully irrigated treatments (FIT) and 25% irrigation treatments (25%FIT), and percent ET_c applied to the of 25% irrigation and 60% irrigation treatment (%ET_c).

	Kimberly, ID – NWISRL				Powell, WY – PREC			
Year	ET_c (mm)	FIT (mm)	25% FIT (mm)	%ET_c (%)	ET_c (mm)	FIT (mm)	60% FIT (mm)	%ET_c (%)
2014	662	712	-	-	-	-	-	-
2015	657	652	237	36	-	-	-	-
2017	645	788	322	50	-	-	-	-
2018	756	803	321	42	563	500	352	63

2.3.2. PREC - Powell, WY

Irrigation scheduling for the FIT was based on balancing estimated cumulative weekly crop ET with the weekly cumulative irrigation and precipitation. Estimated crop ET was based on the ASCE standardized reference evapotranspiration equation (ASCE, 2005) and daily crop coefficients (Wright, 1982) using daily climatic data from a PREC weather station (Sharma et al., 2018). Irrigation was applied weekly with the amount depending upon weekly ET rate and precipitation. Soil water content was measured in 0.3 m depth increments from 0.3 to 0.9 m using neutron probe calibrated to site conditions. Soil water content was monitored in two replicated blocks. Soil water content was measured periodically throughout the growing season to avoid water stress in the fully irrigated treatments by ensuring that available soil water content remained greater than 45% of total available moisture (Jensen et al., 1990). Estimated well-watered sugarbeet ET between emergence and harvest, cumulative irrigation between emergence and harvest applied to the FIT and 25% FIT treatments at PREC are given in Table 1. Estimated well-watered sugarbeet ET was 83% of the 4-yr average at NWISRL due to of lower mean R_s and VPD and higher mean RH at PREC.

2.4. Instrumentation

One infrared radiometer (SI-121, Apogee Instruments, Logan, UT) was installed in each monitored irrigation treatment plot to measure T_c after the sugarbeet crop reached full cover. The radiometers were installed at a height of 0.5 m above the canopy and pointed northeasterly approximately 45° from nadir with the field of view aimed at sunlit canopy surface. The height and view of the radiometers were routinely checked and adjusted as necessary. Climatic parameters R_s (SP-110 pyranometer, Apogee Instruments, Logan, UT), T_a, RH (HMP50 temperature and humidity probe, Campbell Scientific, Logan, UT), and WS (034B, Met One Instruments, Inc., Grants Pass, OR) at 2 m height were measured adjacent to the experimental plots. Canopy temperatures and climatic parameters were measured every minute from mid-July through mid-September of each year with a data logger (CR1000, Campbell Scientific, Logan, UT) and recorded as 15-min averages.

Average climatic parameters measured between 13:00 and 16:00 MDT for both study sites are summarized in Table 2. The climatic conditions at the study sites were similar, which was expected since both are arid mid-latitude western U.S. locations. Solar radiation at PREC was more variable than NWISRL due to the greater prevalence of partly cloudy conditions resulting in a lower mean value and greater standard deviation. Air temperature and WS at both sites were very similar. Mean RH at PREC was greater than NWISRL. Mean VPD at PREC was less than for NWISRL due to the combination of differences in T_a and RH between the study sites. Collectively, the two experimental sites provided a wide range in VPDs needed for robust data-driven model development.

2.5. Data Analysis

The integrity of measured canopy temperature data was verified to include only dry canopy conditions in the dataset used for T_{LL} and T_{UL} model development and evaluation. This was accomplished by omitting canopy temperature data for times of suspected wet canopy conditions based on rain gauge data and irrigation records. Data used in this study was limited to 13:00 to 16:00 MDT, which corresponds to about -1 to +2.5 hours of solar noon for the study sites. Models to estimate T_{LL} and T_{UL} used data from this time interval in their development. Consequently, model predictions are limited to this time frame as well.

A neural network model was used to estimate T_{LL} for each 15-min period between 13:00 and 16:00 MDT based on measured 15-min average climatic conditions. Neural network model development was conducted using MATLAB Neural Network Toolbox (MathWorks, Natick, MA). The dataset was randomly subdivided into one of three

Table 2
Minimum (min), maximum (max), mean and standard deviation (std dev) of 15-min averaged climatic values measured at 1-min intervals between 13:00 and 16:00 MDT at both study sites.

	Kimberly, ID – NWISRL				Powell, WY – PREC			
Climatic Parameter	min	max	mean	std dev	min	max	mean	std dev
Solar Radiation (W m^{-2})	28	1120	749	180	22	1079	675	258
Air Temperature (°C)	8	36	26	5	11	37	26	5
Relative Humidity (%)	7	85	29	12	10	89	32	15
Wind Speed (m s^{-1})	0.3	8.6	2.6	1.1	0.6	8.2	2.6	1.1
Vapor Pressure Deficit (kPa)	0.2	5.3	2.6	1.0	0.3	4.0	2.1	0.8

datasets used to train, validate, and test the NN model. Fifty percent of the dataset was used for training, 25% for validation and 25% for testing. Model parameters (R_s, T_a, RH, WS, T_c) were linearly scaled to a range of −1 to 1 based on measured maximum and minimum values, which is a standard procedure to facilitate convergence to NN model solution, and the Levenberg-Marquardt backpropagation method was used to solve for model coefficients (MATLAB Neural Network Toolbox, MathWorks, Natick, MA). A multilayer perceptron feed forward NN architecture was used to estimate canopy temperature of well-watered sugarbeet. Hidden layer neurons used a hyperbolic tangent activation function and the single output neuron used a linear activation function. The number of hidden neurons was selected by trial and error based on minimizing sum of squared errors between measured and predicted T_{LL}, while using a minimum number of neurons to reduce risk of over-training the NN model to the dataset.

Equation 1 was used to solve for T_{UL} in each 15-min period between 13:00 and 16:00 MDT based on measured 15-min average climatic conditions. Calculation of meteorological parameters Δ and ρ in equations 1 and 2 and VPD followed procedures given in ASCE (2005). The value for c_p in equation 1 was taken as 1013 J kg^{-1} $°C^{-1}$. Net radiation was not directly measured in any study year but calculated from measured 15-min averaged data collected at PREC in 2017 as part of a Bowen Ratio study in sugarbeet. The linear relationship between measured R_n and R_s at PREC was $R_n = 0.65^*R_s + 14.7$ with an R^2 = 0.95.

The CWSI for a 15-min period between 13:00 and 16:00 MDT was calculated using model predicted values for T_{LL} and T_{UL} based on 15-min average measured values for R_s, T_a, RH, WS, and T_c. A daily CWSI value was calculated as the average of the twelve 15-min computed CWSI values between 13:00 and 16:00 MDT.

Linear and multiple linear regression was conducted using MS Excel data analysis tools. Graphical, linear and multiple linear regression were used to quantify performance of prediction models. Regression line significance was evaluated using ANOVA (p ≤ 0.05). Graphs were generated using Sigmaplot 13 (Systat Software, San Jose, CA).

2.5.1. Model evaluation

The effectiveness of model predictions for T_{LL} was accessed using four goodness of fit measures: Nash-Sutcliffe mode efficiency (NSE), mean absolute error (MAE), root mean squared error (RMSE), and percent bias (PBIAS).

The NSE is a normalized statistic that expresses the relative magnitude of the residual variance to measured data variance (Nash and Sutcliffe, 1970). It is defined as:

$$NSE = 1 - \frac{\sum (O_i - P_i)^2}{\sum (O_i - \overline{O})^2} \tag{3}$$

where P_i is the model prediction for a measured value (O_i) and $\overline{O}$ is the mean of the measured values. The NSE assesses the predictive efficacy of a model and can range from −∞ to 1 where a value of 1 means $P_i = O_i$ for all measured data. A value nearer 1 denotes better model prediction efficacy. A negative value denotes the mean of the observations is a better predictor of O_i than the model.

The MAE quantifies the average magnitude of model prediction error absolute values. It is defined as:

$$MAE = \frac{\sum |P_i - O_i|}{n} \tag{4}$$

where n is the number of observations. A smaller MAE indicates better model prediction performance.

The RMSE is the sample standard deviation of the differences between predicted and observed values. It is defined as:

$$RMSE = \sqrt{\frac{\sum (P_i - O_i)^2}{n}} \tag{5}$$

A smaller RMSE indicates better model prediction performance.

The PBIAS is a measure of how much the fitted model over or under predicted the observed values. The PBIAS was calculated as (Yapo et al., 1996):

$$PBIAS = \left[\frac{\sum (P_i - O_i)}{\sum O_i}\right] * 100 \tag{6}$$

Values for PBIAS range from -∞ to ∞ with an optimal value of zero; however, values close to zero can occur if the fitted model overpredicts as much as it underpredicts (Moriasi et al., 2007).

3. Results

3.1. Soil water status

3.1.1. NWISRL - Kimberly, ID

Begin and end of season soil water profiles for FIT and 25%FIT treatments in study years 2015, 2017 and 2018 are shown in Fig. 1. Nominal field capacity and permanent field capacity for the Portneuf silt loam soil at study NWISRL is 32% and 14% by volume as determined in the laboratory using a pressure plate apparatus (McDole et al., 1974). In this study, field capacity and permanent wilting point were taken as the maximum and minimum soil water contents measured during the study, which generally occurred at the beginning and end of the season (Fig. 1). Based on measured soil water contents, field capacity and permanent wilting point were estimated to be 36% and 9%, respectively. The real behavior of crops often reveals that soil water can be extracted below the classical soil water potential threshold of -1.5 MPa (Cabelguenne and Debaeke, 1998). Based on observed values of field capacity and permanent wilting point, maintaining 45% available soil water to avoid crop water stress corresponds to 21% soil water content. Soil water profiles for the FIT treatment in all study years at NWISRL 1 (Fig. 1) demonstrate that cumulative water inputs replenished sugarbeet ET over the growing season as there was little difference in soil profile water content between sampling dates and a major portion of the soil water profile in the FIT treatments remained greater than 21% soil water content at the end of the season and throughout the season (data not shown). Sugarbeet in 25%FIT extracted nearly all available soil water to a depth of 1.2 m over the season. Soil water was extracted below 2 m in each study year in 25%FIT. However, soil water extraction below 1.5 m was limited, likely due to limited root

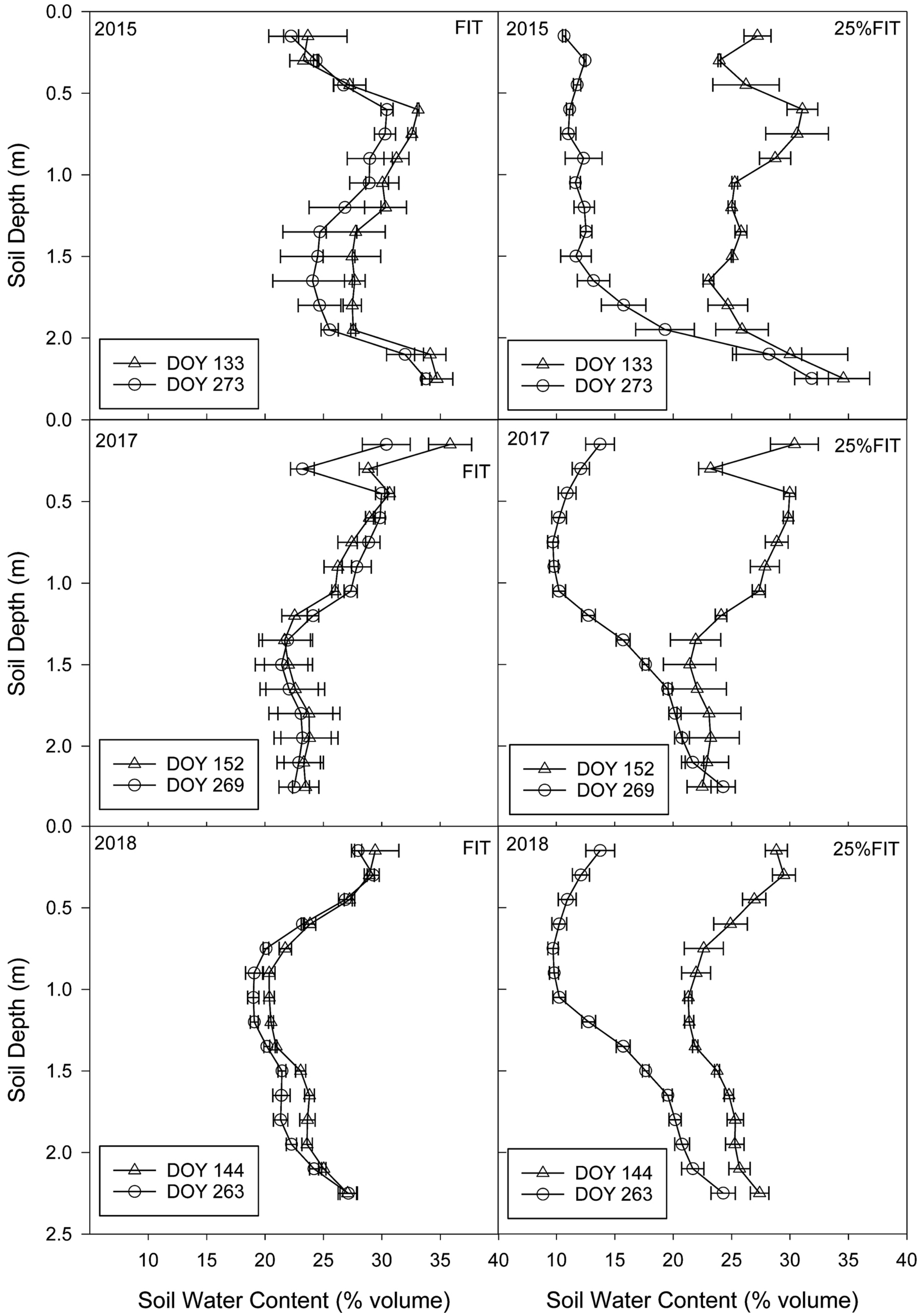

Fig. 1. Beginning and end of season soil water content profiles for sugarbeet FIT (fully irrigated) and 25%FIT treatments for years 2015, 2017 and 2018 at study Kimberly, ID (NWISRL). Bars represent standard error of the measurements.

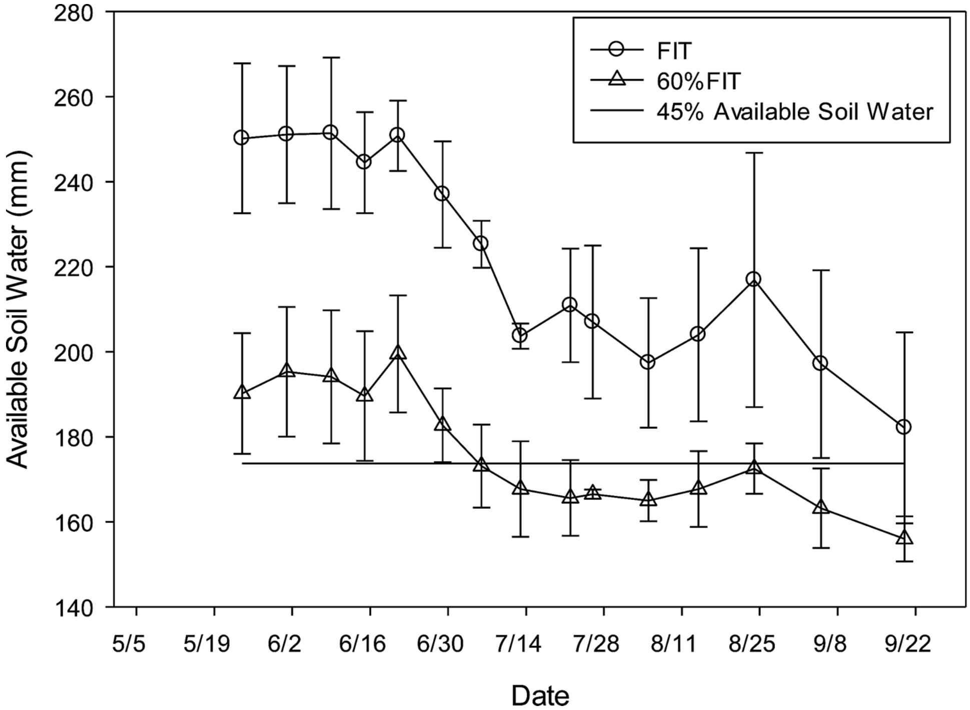

Fig. 2. Total available soil water in 0.9 m soil profile between sugarbeet emergence and harvest for FIT and 60%FIT treatments at study Powell, WY (PREC) in 2018. Bars represent standard error of the measurements.

mass below 1.5 m.

3.1.2. PREC - Powell, WY

Total available soil water over the growing season at PREC is shown in Fig. 2. Soil water measurement was limited to 0.9 m due to prevalence of stones in the lower soil profile. Based on soil texture and observed soil water contents in previous studies at the field site, field capacity and permanent wilting point were estimated to be 27% and 13%, respectively. Available soil water decreased rapidly in the FIT plots due to irrigation water supply system failure the last week in June. Soil water in the 60%FIT was below the 45% depletion limit soon after irrigation system failure and remained below the limit throughout the remainder of the season.

3.2. Well-watered canopy temperature dataset

The study sites had a wide range in climatic conditions leading to a wide range in vapor pressure deficits (Table 2) and measured well-watered canopy temperatures. The linear correlation between $T_c - T_a$ and VPD measured between 13:00 and 16:00 MDT is significant ($p \leq 0.001$) with a correlation coefficient of 0.70 (Fig. 3). The NSE, RMSE, MAE, and PBIAS of the linear regression model were 0.70, 1.65 °C, 1.27 °C, and 0, respectively. The significant linear relationship is consistent with the linear behavior of the canopy temperature model of Idso et al. (1981) and Jackson et al. (1981). A second order model does not improve $T_c - T_a$ prediction despite the appearance of dataset nonlinearity for high and low VPD. The high degree of variability for $T_c - T_a$ at any given value of VPD illustrates a strong influence of additional factors on leaf temperature other than soil water availability. The small grouping of data values above the bulk data at VPD ~3.7 kPa occurred during a high wind event exceeding 6 m s^{-1} at NWISRL, which may have decreased stomatal conductance (Davies et al., 1978; Renard and Demessemacker, 1983; Kobriger et al., 1984; Campbell-Clause, 1998) reducing transpiration rate and increasing canopy temperature despite adequate soil water availability.

3.3. Model prediction of T_{LL}

The NN model developed to predict T_{LL} using input variables T_a, R_s, RH, and WS measured between 13:00 and 16:00 MDT was significant ($p \leq 0.001$) with a correlation coefficient of 0.88 between measured and predicted T_{LL} (Fig. 4). The NN model used only four hidden neurons. The NSE, RMSE, MAE, and PBIAS of the NN model were 0.88, 1.07 °C, 0.82 °C, and 0, respectively. The NN model prediction performance is a substantial improvement to the linear model with VPD (Fig. 3). Linear regression equation slope for predicted versus measured T_{LL} was significantly different ($p < 0.001$) (0.87, Fig. 4) from one indicating a bias in predictions. The NN model over-predicts T_{LL} for temperatures < 20 °C and under-predicts for temperatures > 25 °C despite a PBIAS = 0.

3.4. Model for estimating T_{UL}

The dataset used to determine the linear relationship between $\bar{T_c} - \bar{T_a}$ and VPD for estimating average canopy aerodynamic resistance ($\bar{r_{ap}}$) (Eqn. 2) is depicted in Fig. 5. The difference between the datasets in Fig. 3 and Fig. 5 was the removal of $T_c - T_a$ for Rs < 750 W m^{-2} to eliminate the possible inclusion of data where canopy resistance was increased due to reduced sunlight and actual ET was less than potential ET. Data values for high wind conditions (WS > 5.5 m s^{-1}) were also removed to eliminate the possible influence of high wind on canopy resistance. Linear regression of the dataset (Fig. 5) R^2 = 0.85 ($p < 0.001$) resulted in a slope of 3.02 °C kPa^{-1} and intercept of 4.92 °C. Dataset (Fig. 5) values for $\bar{\Delta}$, $\bar{\gamma}$, and $\bar{\rho}$ were 212.8 Pa °C^{-1}, 60.6 Pa °C^{-1}, and 1.05 kg m^{-3}, respectively. The linear relationship between R_s and R_n was used to calculate R_n from measured 15-min averaged values of R_s for both sites. Based on this relationship, the dataset (Fig. 5) value for $\bar{R_n}$ was 573 W m^{-2}. Substituting dataset average values into Eqn. 2 resulted in $\bar{r_{ap}}$ = 25.4 s m^{-1}. Substituting the appropriate values into Eqn. 1 resulted in T_{UL}–T_a = 13.7 °C. These values are quite sensitive to the slope and intercept of the regression equation through the dataset. The range in T_{UL}–T_a corresponding to the 95% confidence interval for the slope (-2.96, -3.07) of the regression line for the dataset (Fig. 5) was

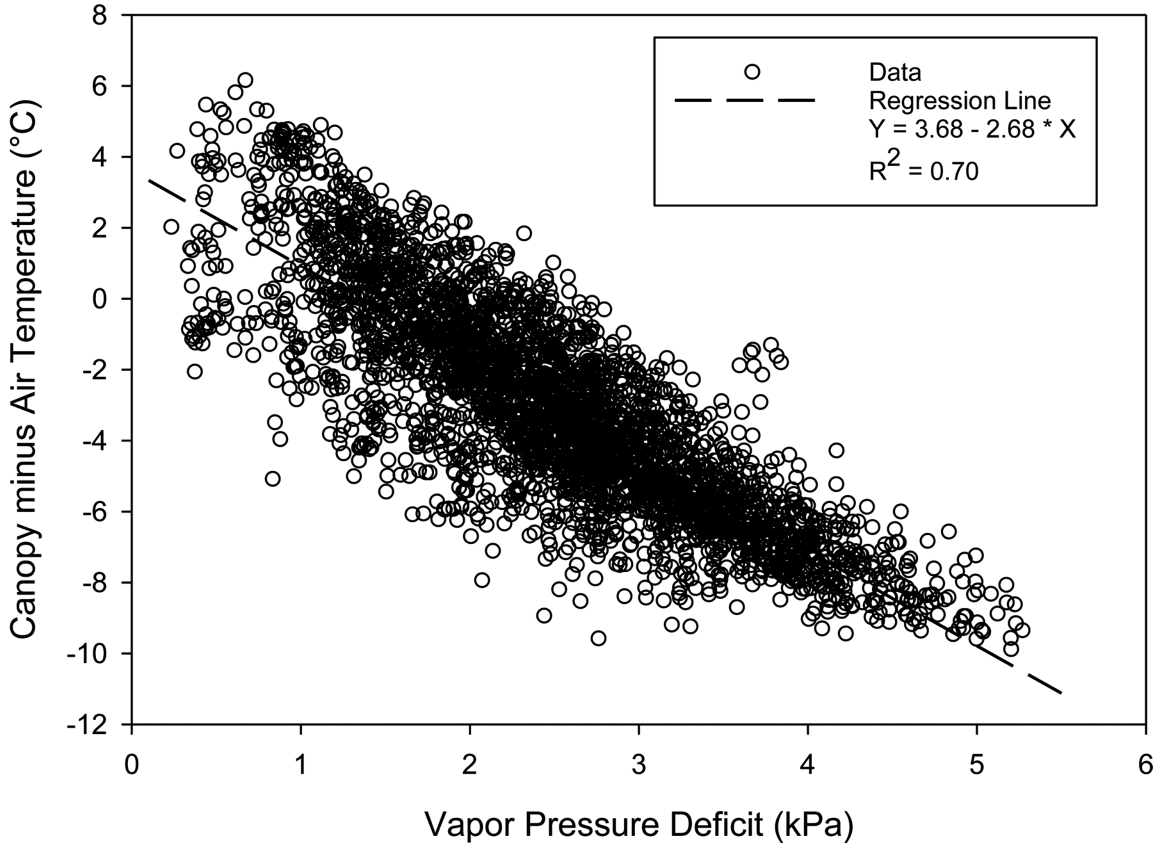

Fig. 3. Relationship between canopy temperature minus air temperature and vapor pressure deficit for well-watered sugarbeet measured between 13:00 and 16:00 MDT at both experimental sites in all years (n = 3386).

12.9 to 14.6 °C. Using sugarbeet canopy temperature data from Idso (1982), O'Toole and Real (1986) calculated $\bar{r}_{ap}$ = 8.8 s m^{-1}, which leads to T_{UL}–T_a of about 4.5 °C, substantially less than 13.7 °C obtained in this study. The dataset of Idso (1982) was comprised of 47 data values over a VPD range of 1.5 to 4.1 kPa resulting in a regression slope of -1.96 °C kPa^{-1}, much less than the slope found in this study using over 3,000 data values spanning a larger range in VPD. The dataset of Sepaskhah et al. (1988) was comprised of 77 values over a VPD range of 1.4 to 4.8 kPa resulting in a regression slope of -2.6 °C kPa^{-1}, which for the average values of this study resulted in T_{UL}–T_a =8.5 °C. The datasets of Idso (1982) and Sepaskhah et al. (1988) are enveloped within the dataset collected in this study (Fig. 3). The sensitivity of T_{UL}–T_a to regression line slope underscores the need for a large dataset over a wide range of VPDs to obtain a reliable estimate of T_{UL}–T_a using the approach of O'Toole and Real (1986). Data over a limited range in VPD is not adequate for reliable estimation of T_{UL}–T_a on a regional scale. The regression line slope is very sensitive to data for VPD < 1.5 kPa.

Measured T_c-T_a versus VPD for R_s > 750 W m^{-2} (Fig. 5) diverges from a linear relationship for VPD < 1.0 kPa and VPD > 4.5 kPa indicating the linear canopy temperature model of Idso et al. (1981) and Jackson et al. (1981) may not apply for all VPD. A quadratic equation provides a better fit (R^2 = 0.86, not shown) to the data than a linear equation. When VPD is < 1.0 kPa the vapor pressure gradient across the leaf surface boundary begins to limit latent heat transfer rate causing leaf surface temperature to increase to maintain the energy balance between radiant, latent, and convective heat exchange with the environment. When VPD is > 4.5 kPa latent heat transfer (transpiration) becomes limited by energy availability, limiting cooling and resulting in a lower limit for T_{LL}-T_a. The dataset of Sepaskhah et al. (1988) had a similar trend for VPD > 4.5 kPa.

The cumulative probability distribution of maximum 15-minute values of T_c-T_a measured in the 25%FIT and 60%FIT treatments during the study is shown in Fig. 6. The maximum measured value of T_c-T_a exceeded 15 °C. The value of T_{UL}–T_a (13.7 °C) estimated using the method of O'Toole and Real (1986) is less than the 15 °C but exceeded by only 0.5% of the values measured and appears to be a reasonable estimate of T_{UL}–T_a for the average conditions for $\bar{\Delta}$, $\bar{\gamma}$, $\bar{\rho}$, and $\bar{R}_n$. Coincidently, there is a discontinuity in the data at approximately 13.7 °C. This may be due to the occurrence of sugarbeet wilting when severely water-stressed under high VPDs, potentially resulting in some background soil temperature measurement by infrared radiometers. Maximum measured values for T_c-T_a in deficit irrigated plots exceeded values for T_{UL}–T_a estimated by O'Toole and Real (1986) and Sepaskhah et al. (1988) 20 and 5% of the time, respectively.

3.5. Daily CWSI

3.5.1. NWISRL - Kimberly, ID

Daily CWSI values computed as the average 15-min CWSI between 13:00 and 16:00 MDT are shown in Fig. 7 along with daily irrigation plus precipitation amounts for both study sites. Daily CWSI at NWISRL in 2015 was less than 0.1 before mid-July and rapidly increased and oscillated between 0.2 and 0.4 in response to small frequent irrigation amounts until mid-August. Daily CWSI value then increased to 0.5 by the end of August in response to about a week without irrigation. Daily CWSI decreased to 0.1 in early September in response to precipitation, reduced ET, and irrigation. Daily CWSI then increased to 0.5 by the end of September due to withheld irrigation for a week. Over the season, daily CWSI decreased a limited amount following irrigation due to the small irrigation applications by the lateral-move irrigation system. The minimal reduction in daily CWSI from irrigation may have resulted from a substantial fraction of applied water evaporating from the crop and soil surface rather than entering the soil profile. Daily CWSI at

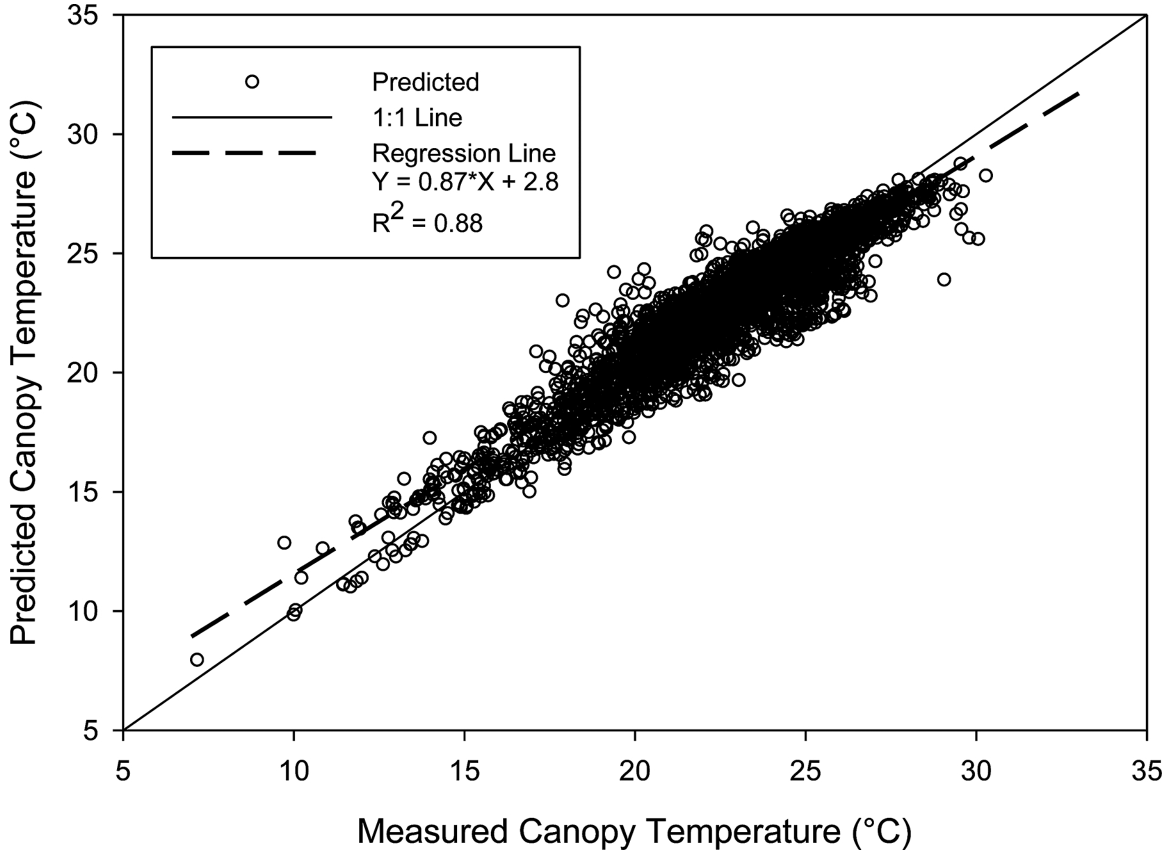

Fig. 4. Neural network (NN) prediction of sugarbeet well-watered canopy temperature compared to measured canopy temperature measured between 13:00 and 16:00 MDT at both experimental sites in all years (n = 3386).

NWISRL in 2017 oscillated between 0.15 and 0.4 for much of the season with a notable decrease to near zero in the beginning of September due to increased irrigation frequency. Daily CWSI increased after the first week in September and varied between 0.15 and 0.4 for the remainder of September. Daily CWSI at NWISRL in 2018 varied between 0.1 and 0.35 until mid-August. Then daily CWSI decreased to zero due to reduced ET from cooler cloudy conditions while irrigation continued largely unchanged in amount and frequency. In early September, daily CWSI increased to about 0.25 when irrigation frequency decreased, then decreased in mid-September when irrigation frequency increased. Daily CWSI was greater in 2015 than either 2017 or 2018 at NWISRL. This is likely due to irrigation plus precipitation applied to the 25%FIT in 2015 being 36% of estimated sugarbeet ET (Table 1) compared to 50 and 42% in 2017 and 2018, respectively.

3.5.2. PREC - Powell, WY

Over the season, daily CWSI of the 60%ET treatment at PREC in 2018 varied between 0 and 0.9 in response to water application (Fig. 7). Daily CWSI was greater than 0.8 in mid-July due to lack of irrigation resulting from the irrigation supply system equipment failure at the end of June. Total available soil water was below 45% available in mid-July (Fig. 2) resulting in daily CWSI exceeding 0.8. Daily CWSI rapidly decreased to less than 0.1 by the end of July due to several irrigations. Soil water content stabilized but did not substantially increase (Fig. 2). In the first week of August daily CWSI rapidly increased to nearly 0.8 when irrigation frequency decreased (Fig. 7). Three irrigations between 18 July and 27 July, which rapidly decreased daily CWSI, likely restored soil water in the top 0.15 m of the soil profile that was not detected by neutron probe soil water measurements. The water stored in the 0.15 m soil profile was readily removed by the sugarbeet crop and daily CWSI rapidly increased during early August following depletion. The two irrigations between 10 August and 15 August stabilized daily CWSI and the two irrigations between 16 August and 20 August decreased daily CWSI to zero and increased total available soil water slightly (Fig. 2). During the first ten days of September, daily CWSI rapidly increased to 0.8 due to the lack of irrigation, which likely depleted soil water in the top 0.15 m of the soil profile and decreased measured soil water content (Fig. 2). Soil water content reached a minimum on 11 September and daily CWSI reached a maximum of 0.9. Daily CWSI at PREC was much more dynamic than for NWISRL due to limited soil water storage resulting from less water holding capacity of the loam soil and a restricted crop root zone.

4. Discussion

The daily CWSI based on predicted values for T_{LL} and T_{UL} by models developed in this study provided a more responsive measure of crop water stress for sugarbeet than soil water monitoring. Daily CWSI at NWISRL (Fig. 7) did not exceed 0.5 despite soil water depletion well below 45% available soil water in the 0 to 1 m soil profile (Fig. 1). Sugarbeet is known to be a deep-rooted crop in an unrestricted soil profile, but a priori knowledge of root zone depth for efficient irrigation scheduling based on soil water monitoring is usually lacking. Additionally, soil water monitoring below 0.6 m is not a common practice due to equipment and/or labor requirements. Sugarbeet soil water extraction readily occurred to a depth of 1.5 m at NWISRL and to a limited extent to a depth of 2 m (Fig. 1). Daily CWSI < 0.5 with 25%FIT irrigation amounts suggests that soil water extraction below 1 m was enough to supplement but not fully supply sugarbeet ET throughout the season. Daily CWSI at PREC was a more responsive indicator of crop water stress than soil water monitoring likely resulting from inadequate representation of soil water storage in the top 0.15 m of the root zone

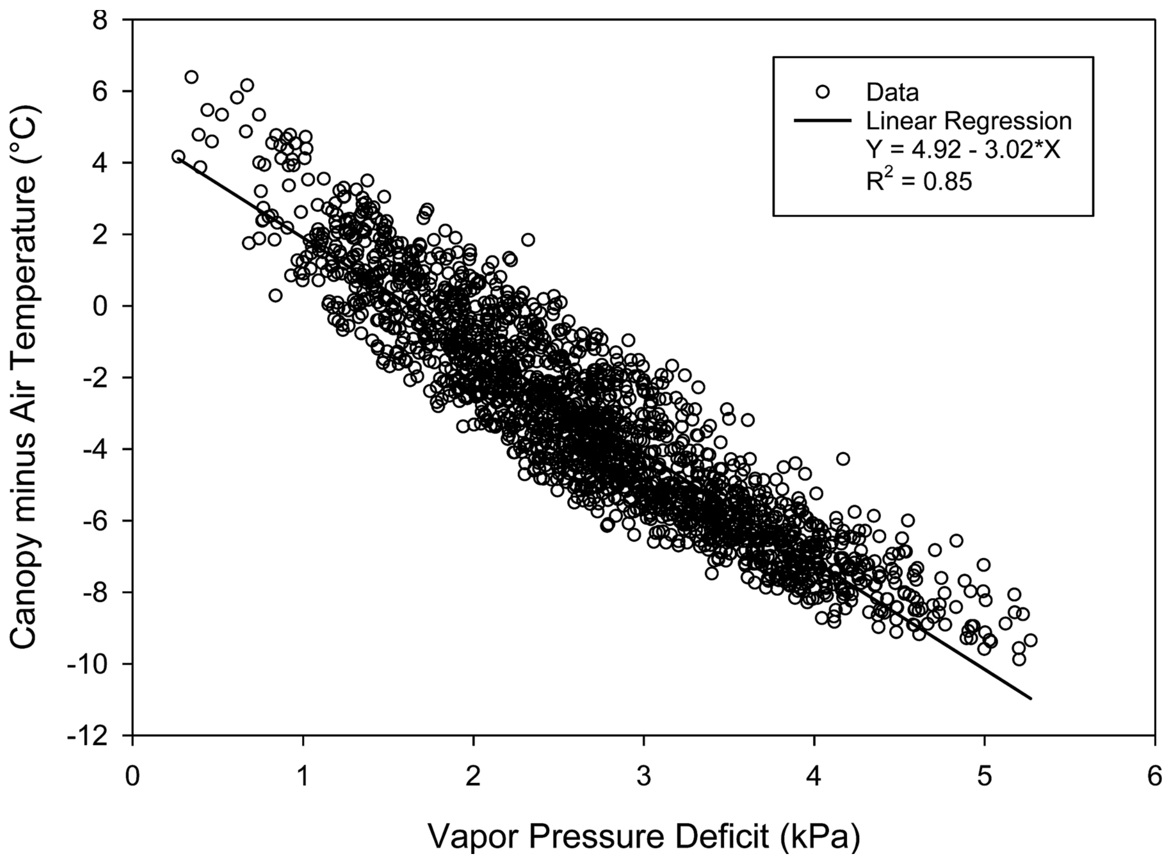

Fig. 5. Relationship between canopy temperature minus air temperature and vapor pressure deficit for well-watered sugarbeet measured between 13:00 and 16:00 MDT at both experimental sites in all years used to estimate average canopy aerodynamic resistance (n = 1989).

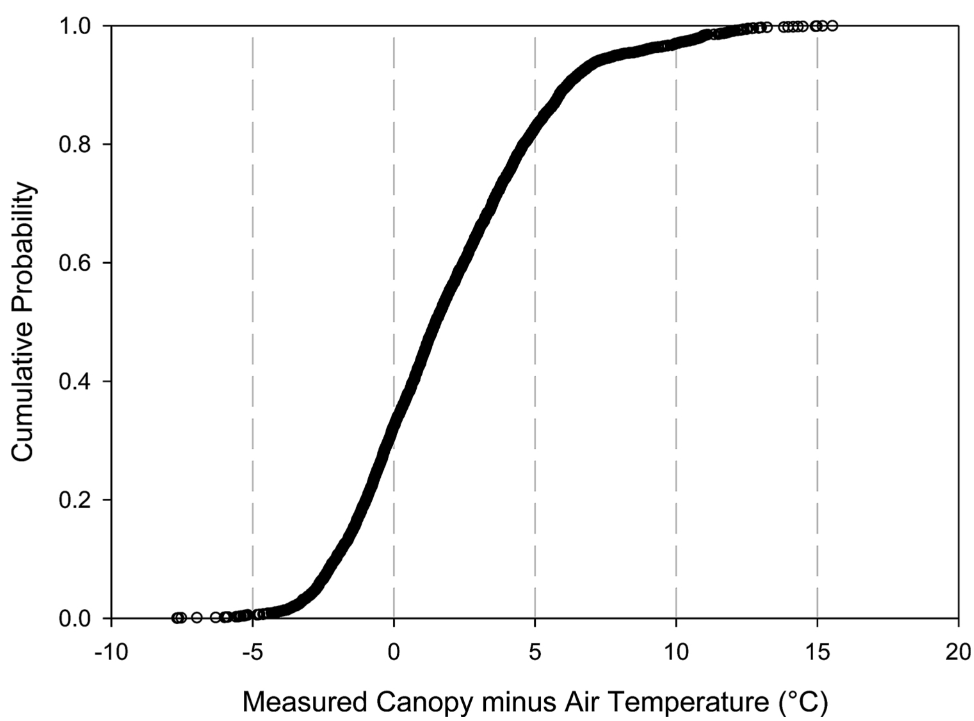

Fig. 6. Cumulative probability distribution of canopy temperature minus air temperature measured between 13:00 and 16:00 MDT at both experimental sites in deficit irrigated treatments during the study.

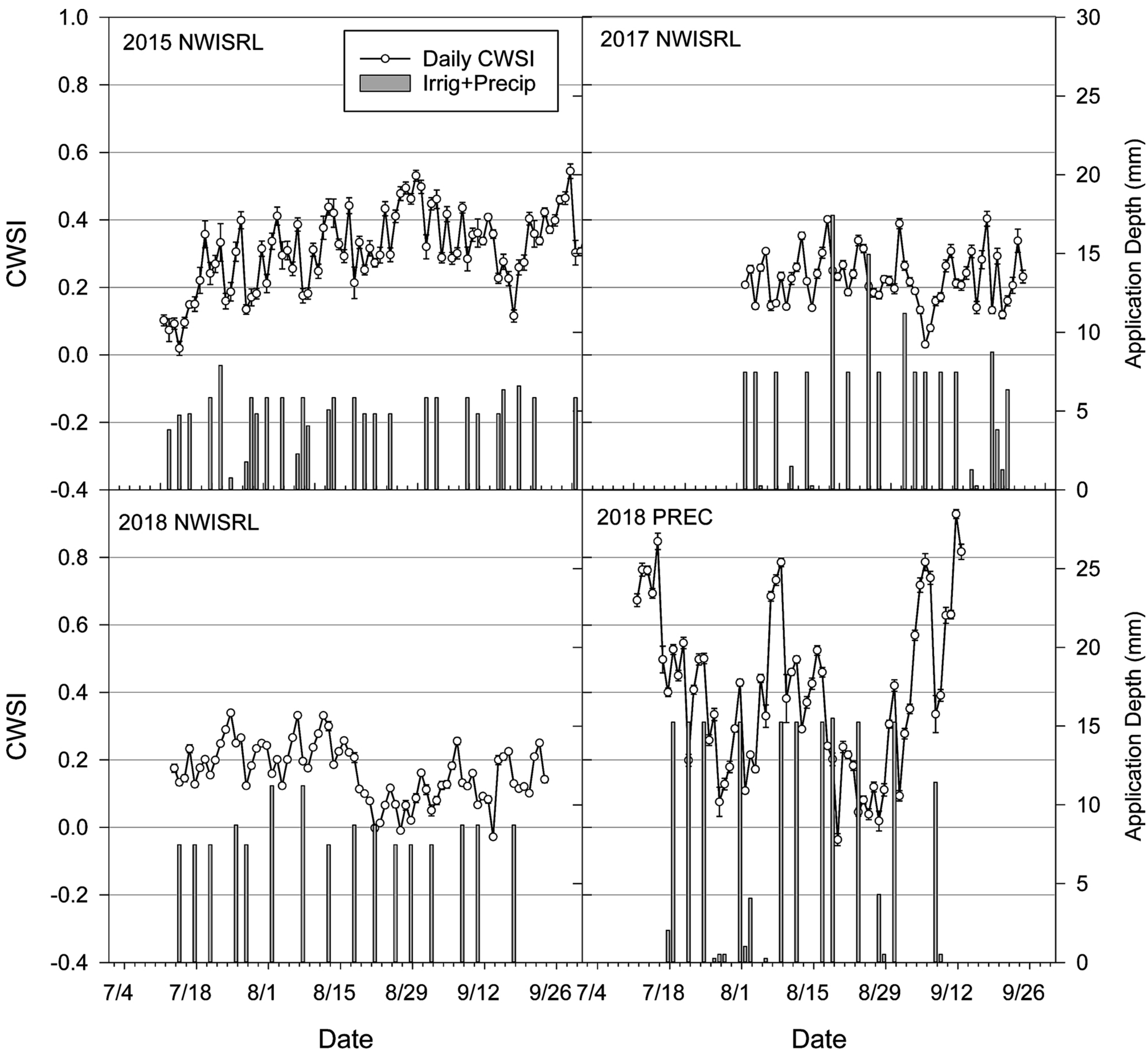

Fig. 7. Sugarbeet crop water stress index and irrigation plus precipitation amounts for 25%FIT (fully irrigated treatments) at Kimberly, ID (NWISRL) and 60%FIT at Powell, WY (PREC). Bars represent standard error of the measurements.

that apparently acted as the primary soil moisture storage reservoir for the 60%FIT. Apparently, when irrigation frequency was enough to maintain some level of soil water availability in the top 0.15 m soil profile daily CWSI was reduced, and when it was depleted daily CWSI was greater than 0.5. Crop water stress assessment using daily CWSI overcomes the uncertainty associated with estimating effective root zone depth needed to assess crop water stress using soil water monitoring, potentially providing a more responsive measure of crop water stress.

Calculation of CWSI using a constant value for T_{UL} (Cohen et al., 2005; Alchanatis et al., 2010; Möller et al., 2007; King and Shellie, 2016) measured on water-stressed plants under high VPD resulted in a CWSI that steadily decreased over the season regardless of soil water content (data not shown). This was attributed to failure to account for the effect of decreasing solar radiation over the season on T_{UL} resulting in over estimation of T_{UL} late in the season. Use of constant T_{UL} also results in a sudden decrease in CWSI value for overcast days with low solar radiation without a corresponding change in soil water status. In this study, calculation of T_{UL} using Eqn. 1 with $\bar{r}_{ap}$ = 25.4 s m^{-1} and calculated 15-min average R_n resulted in CWSI values adjusted for decreasing solar radiation over the season and overcast days. This method for calculating T_{UL} removed the decreasing trend in CWSI over the season regardless of soil moisture status (Fig. 7). However, cloudy days are problematic as small R_n in Eqn. 1 results in a small denominator in calculation of CWSI, which inflates the CWSI. Wet canopy from precipitation or irrigation can result in measured T_c up to several degrees C less than predicted T_{LL} resulting in calculation of a negative CWSI. An example of wet canopy effect on daily CWSI can be viewed in Fig. 6 for PREC on 20 August where daily CWSI was negative and 0.2 less than the preceding or following day. Irrigation scheduling decision support software would need to include filters to suspend activation of automatic irrigation scheduling when these circumstances occur. Despite these potential anomalies in computing CWSI, using the methodology applied in this study to estimate T_{LL} and T_{UL} between 13:00 and 16:00 MDT based on measured meteorological conditions could be used for irrigation scheduling of sugar beets to increase utilization of stored soil water to reduce seasonal irrigation requirements. Irrigation scheduling based on daily CWSI would circumvent the uncertainty associated with estimating soil water holding capacity, critical soil water fraction, and effective crop rooting depth.

In this study, data collected at two sites with differing meteorological conditions, even though both sites were arid, substantially influenced the results of this study. Data values of T_c-T_a for VPDs < 2 kPa were largely from PREC and without PREC data, the results of this study would have been nearly identical to those of Idso (1982) and Sepaskhah et al. (1988). Slope of the regression line for T_c-T_a vs VPD would have been greater (less negative) resulting in a lower value for T_{UL}-T_a. Calculation of daily CWSI would have resulted in greater values for NWISRL but if transferred to PREC would have resulted in CWSI values > 1. The result of this study emphasizes the need for a robust data set of T_c-T_a versus VPD in order to successfully use data driven models to determine baseline temperatures applicable to a large regional basis or worldwide climatic zone. The NN model developed for estimating T_{LL} used 15-min average values of R_s, T_a, RH and WS as inputs and consists of 24 static coefficients. The NN model can be easily implemented in a spreadsheet or embedded in irrigation decision support software.

5. Conclusions and future research

Data-driven models were used to develop estimates of CWSI baseline temperatures, T_{LL} and T_{UL}, for sugarbeet grown in arid regions of western U.S. Five site-years of measured sugarbeet canopy temperature and meteorological conditions allowed development and evaluation of an NN model for estimating T_{LL}. A linear regression driven physical model for estimating T_{UL}-T_a resulted in a value of 13.7 °C for the average meteorological conditions of the study. A value much greater than results from other sugarbeet studies found in the literature but representative of maximum measured T_c-T_a temperature measured in deficit irrigated plots of this study. Daily 3-h average CWSI calculated using 15-min average estimates of T_{LL} and T_{UL} between 13:00 to 16:00 MDT provided more responsive representation of sugarbeet water stress than measured soil moisture in deficit irrigated plots. Using canopy temperature to determine sugarbeet water stress would circumvent problems of estimating soil water holding capacity, allowable soil water depletion, effective rooting depth, and soil water measurement for water balance irrigation scheduling. Additional research should focus on investigating the relationship between daily CWSI and available soil water to allow estimation of needed irrigation application depth based on computed CWSI. The relationship between seasonal CWSI, sugarbeet yield and water use efficiency should be determined for establishing optimum irrigation management based on CWSI.

Declaration of Competing Interest

The authors report no declarations of interest.

Acknowledgements

The use of trade, firm, or corporation names in this article is for the information and convenience of the reader. Such use does not constitute an official endorsement or approval by the United States Department of Agriculture or the Agricultural Research Service of any product or service to the exclusion of others that may be suitable. The USDA is an equal opportunity provider and employer. This research did not receive any specific grant from funding agencies in the public, commercial, or not-for-profit sectors. Declaration of interests: none.

Appendix A. Supplementary data

Supplementary material related to this article can be found, in the online version, at doi:https://doi.org/10.1016/j.agwat.2020.106459.

References

ASCE, 2005. The ASCE standardized reference evapotranspiration equation. Environmental and Water Resources Institute of the American Society of Civil Engineers final report. Reston, VA. Accessible at: https://epic.awi.de/id/eprint/42362/1/ascestzdetmain2005.pdf (accessed 6 May 2019). .
Alchanatis, V., Cohen, Y., Cohen, S., Möller, M., Sprinstin, M., Meron, M., Tsipris, J., Saranga, Y., Sela, E., 2010. Evaluation of different approaches for estimating and mapping crop water status in cotton using thermal imaging. Precis. Agric. 11 (1), 27–41.
Bockhold, D.L., Thompson, A.L., Sudduth, K.A., Henggeler, J.C., 2011. Irrigation scheduling based on canopy temperature for humid environments. Trans. ASABE 54 (6), 2021–2028.
Cabelguenne, M., Debaeke, P., 1998. Experimental determination and modelling of soil water extraction capacities of crops of maize, sunflower, soya bean, sorghum and wheat. Plant and Soil 202 (2), 175–192.
Campbell-Clause, J.M., 1998. Stomatal response of grapevines to wind. Australian J. Expr. Ag. 38 (1), 77–82.
Cohen, Y., Alchanatis, V., Meron, M., Saranga, Y., Tsipris, J., 2005. Estimation of leaf water potential by thermal imagery and spatial analysis. J. Exp. Bot. 56 (417), 1843–1852.
Davies, W.J., Gill, K., Halliday, G., 1978. The influenc of wind on the behavior of stomata of photosynthetic stems of *Cytisus scoparius* (L.) link. Ann. Bot. 42 (5), 1149–1154.
Dunham, R.J., 1993. Water use and irrigation. In: Cooke, D.A., Scott, R.K. (Eds.), The Sugar Beet Crop: Science into Practice. Chapman & Hall, London, pp. 279–309.
Han, M., Zhang, H., Chavez, J.L., Ma, L., Trout, T.J., DeJonge, K.C., 2018. Improved soil water deficit estimation through integration of canopy temperature measurement into a soil water balance model. J. Irrig. Sci. 36 (3), 187–201.
Hignett, C., Evett, S.R., 2002. Neutron thermalization. In: Dane, J.H., Topp, G.C. (Eds.), Methods of Soil Analysis. Part 4. Physical Methods. SSSA, Madison, WI, pp. 501–521.
Idso, S.B., 1982. Non-water-stressed baselines: A key to measuring and interpreting plant water stress. Agric. Meteorol. 27, 59–70.
Idso, S.B., Jackson, R.D., Pinter Jr., P.J., Reginato, R.J., Hatfield, J.L., 1981. Normalizing the stress-degree-day parameter for environmental variability. Agric. Meteorol. 24, 45–55.
Irmak, S., Haman, D.Z., Bastug, R., 2000. Determination of crop water stress index for irrigation timing and yield estimation of corn. Agron. J. 92 (6), 1221–1227.
Jackson, R.D., Idso, S.B., Reginato, R.J., Pinter Jr., P.J., 1981. Canopy temperature as a drought stress indicator. Water Resour. Res. 13, 651–656.
James, L.G., 1988. Principles of Farm Irrigation System Design. John Wiley & Sons, NY.
Jensen, M.E., Burman, R.D., Allen, R.G., 1990. Evapotranspiration and Irrigation Water Requirements. In: ASCE Manuals and Reports on Engineering Practices no. 70. Am. Soc. Civil Eng. Reston, VA..
Jones, H.G., 1999. Use of infrared thermometry for estimation of stomatal conductance as a possible aid to irrigation scheduling. Agric. For. Meteorol. 95, 139–149.
Jones, H.G., 2004. Irrigation scheduling: advantages and pitfalls of plant-based methods. J. Exp. Bot. 55 (407), 2427–2436.
Jones, H.G., Stroll, M., Santos, T., de Sousa, C., Chaves, M.M., Grant, O.M., 2002. Use of infrared thermography for monitoring stomatal closure in the field: application to grapevine. J. Exp. Bot. 53 (378), 2249–2260.
King, B.A., Shellie, K.C., 2016. Evaluation of neural network modeling to predict non-water-stressed leaf temperature in wine grape for calculation of crop water stress index. Agic. Water Manag. 167, 38–52.
Kobriger, J.M., Kliewer, W.M., Lagier, S.T., 1984. Effects of wind on water relations of several grapevine cultivars. Am. J. Enol. Vitic. 35 (3), 164–169.
Leinonen, I., Jones, H.G., 2004. Combining thermal and visible imagery for estimating canopy temperature and identifying plant stress. J. Exp. Bot. 55 (401), 1423–1431.
Maes, W.H., Steppe, K., 2012. Estimating evapotranspiration and drought stress with ground-based thermal remote sensing in agriculture: a review. J. Exp. Bot. 63, 4671–4712.
Martin, E.C., Stephens, W., Wiedenfeld, R., Bittenbender, H.C., Beasley Jr., J.P., Moore, J.M., Neibling, H., Gallian, J.J., 2007. Sugar, oil and fiber. In: Lascano, R.J., Sojka, R.E. (Eds.), Irrigation of Agricultural Crops. Agron. Monogr. 30. ASA, Madison, WI, pp. 279–335.
McDole, R.E., McMaster, G.M., Larsen, D.C., 1974. Available water-holding capacities of soils in southern Idaho. CIS 236. Univ. of Idaho, Moscow, ID.
Melvin, S.R., Yonts, C.D., 2009. Irrigation scheduling: Checkbook method. (accessed 29 April 2020). http://extensionpublications.unl.edu/assets/pdf/ec709.pdf.
Möller, M., Alchanatis, V., Cohen, Y., Meron, M., Tsipris, J., Naor, A., Ostrovsky, V., Sprinstin, M., Cohen, S., 2007. Use of thermal and visible imagery for estimating crop water status of irrigated grapevine. J Exp. Bot. 58 (4), 827–838.
Moriasi, D.N., Arnold, J.G., Van Liew, M.W., Bingner, R.L., Harmel, R.D., Veith, T.L., 2007. Model evaluation guidelines for systematic quantification of accuracy in watershed simulations. Trans. ASABE 50 (3), 885–900.
Nash, J.E., Sutcliffe, J.V., 1970. River flow forecasting through conceptual models of principles. J. Hydrol. 10 (1), 282–290.
O'Shaughnessy, S.A., Evett, S.R., Colaizzi, P.D., Howell, T.A., 2011. Using radiation thermography and thermometry to evaluate crop water stress in soybean and cotton. Agic. Water Manag. 98, 1523–1535.
O'Toole, J.C., Real, J.G., 1986. Estimation of aerodynamic and crop resistances from canopy temperature. Agron. J. 78, 305–310.
Payero, J.O., Irmak, S., 2006. Variable upper and lower crop water stress index baselines for corn and soybean. Irrig. Sci. 25, 21–32.
Pou, A., Diago, M.P., Medrano, H., Baluja, J., Tardaguila, J., 2014. Validation of thermal indices for water status identification in grapevine. Agric. Water Manag. 134, 60–72.

Raschke, K., 1960. Heat transfer between the plant and the environment. Annu. Rev. Plant Physiology 11, 111–126.
Renard, C., Demessemacker, W., 1983. Effects of wind velocity on stomatal conductance and consequences leaf rolling on water uptake of tall fescue. Biologia Plantarum 25 (6), 408–411.
Sepaskhah, A.R., Nazemossadat, S.M.J., Kamgar-Haghighi, A.A., 1988. Estimation of upper limit canopy to air temperature differential for sugarbeet using indirect measurement of turgor potential. Iran Agricultural Research 7, 107–122.
Sharma, V., Nicholson, C., Bergantino, T., Cowley, J., Hess, B., Tanaka, J., 2018. Wyoming Agricultural Climate Network (WACNet). Univ. of Wyoming, Agricultural Experiment Station Bulletin, Laramie, WY, pp. 52–53.
Tanner, C.B., 1963. Plant temperatures. Agron. J. 55, 210–211.
Winter, S.R., 1980. Suitability of sugarbeets for limited irrigation in a semi-arid climate. Agron. J. 72 (1), 118–123.
Wright, J.L., 1982. New evapotranspiration crop coefficients. J. Irrig. Drain. 108, 57–74.
Withers, B., Vipond, S., 1980. Irrigation Design and Practice. Cornell University Press, Ithaca, NY.
USDA, 1998. Natural Resource and Conservation Service. Soil Survey of Jerome and Part of Twin Falls County, Idaho. Accessible at: https://www.nrcs.usda.gov/wps/portal/nrcs/surveylist/soils/survey/state/?stateId=ID (accessed 10 June 2019). .
USDA, 2019. USDA Web Soil Survey. Accessible at: https://websoilsurvey.nrcs.usda.gov/app/ (accessed 10 June 2019). .
Vellidis, G., Tucker, M., Perry, C., Kvien, C., Bednarz, C., 2007. A real-time smart sensor array for irrigation scheduling. Comput. Electron. Ag. 61, 44–50.
Yapo, P.O., Gupta, H.V., Sorooshian, S., 1996. Automatic calibration of conceptual rainfall-runoff models: sensitivity to calibration data. J. Hydrol. 181, 23–48.